International Journal of Heat and Mass Transfer 52 (2009) 1802–1810

Contents lists available at ScienceDirect

International Journal of Heat and Mass Transfer

journal homepage: www.elsevier.com/locate/ijhmt

Performance evaluation of mixed convection in an inclined square channel with uniform temperature walls

Koichi Ichimiya [a,*], Yasuhiro Matsushima [b]

[a] Interdisciplinary Graduate School of Medicine and Engineering, Mechanical Systems Engineering, University of Yamanashi, 4-3-11 Takeda, Kofu, Yamanashi 400-8511, Japan
[b] Dihatsu Diesel Co. Ltd., 2-4-14 Tokui, Chuoku, Osaka 540-0025, Japan

ARTICLE INFO

Article history:
Received 18 January 2008
Received in revised form 23 July 2008
Available online 8 December 2008

Keywords:
Mixed convection
Inclined square channel
Numerical calculation
Thermal performance

ABSTRACT

Numerical analyses were performed for the effect of inclined angle on the mixing flow in a square channel with uniform temperature walls (T_w = 30 °C) and inlet temperature (T_0 = 10 °C). Three-dimensional governing equations were solved numerically for Re = 100, Pr = 0.72 and various inclined angles (from −90° to 90°). Three-dimensional behavior of fluid in a channel was examined for each angle. Thermal performance was evaluated using the relationship between Nusselt number ratio and pressure loss ratio with and without buoyancy induced flow as a parameter of inclined angles. High heat transfer and low pressure loss region was from −15° to −60° in thermal performance using mean Nusselt number ratio.

1. Introduction

Mixed convection, in which forced and natural convection coexist, is important in laminar flow with compactness of heat transfer device. The attitude of flow passage is one of the most important factors which affect mixed convection. Iqbal and Stachiewicz [1] showed numerical results that heat transfer of inclined tube takes the peak at the region from 20° to 60°. Maughan and Incropera [2] presented that onset of instability was delayed by decreasing the *Gr and/or* by increasing the *Re* and the inclination angle and heat transfer enhancement occurred prior to onset of the secondary flow. Ramachandran and Armaly [3] arranged the patterns on local and average heat transfer corresponding to the direction of the main flow and buoyancy force and the Richardson numbers in a parallel plate duct with uniform wall temperatures. Naito and Nagano [4] showed how the developing upward flow and thermal field in the entry region were affected by buoyancy on friction factor and Nusselt number for various inclination angles of parallel plates. Wikem [5] expressed the map of the relation between friction and heat transfer for various inclination angles in semi-infinite flat plate, either heated or cooled. Choi and Ortega [6] investigated numerically for a parallel planes channel with a discrete heat source, and results indicated that the overall Nusselt number of the source strongly depended on the inclination angle over 45°. Wang and Robillard [7] studied fully developed opposing mixed convection of inclined channel with discrete heating and numerical results revealed that buoyancy effects produced an overall recirculating flow. Yan [8] analyzed numerically the developing laminar mixed convection heat transfer including mass transfer. Galanis [9] evaluated heat transfer characteristics of inclined tube for various heat transfer boundary conditions. Stability of mixed convection in an inclined channel was examined on the generation of a small vorticity by Abu-Mulaweh et al. [10], the dependence of inclination angle by Lee et al. [11], the linear stability theory in a parallel plate duct by Lavine [12] and the secondary flow structure of two or four vorticities by Galanis and Nguyen [13]. Lavine [14] and Lin and Lin [15] indicated the periodicity of temperature change in a reverse flow and the flow visualization of a vorticity or a reverse flow in a slightly inclined rectangular duct, respectively. Morcos et al. [16], Chen et al. [17] and Armaly et al. [18] arranged quantitatively the heat transfer of an inclined rectangular duct with uniform heat flux, inclined plates with constant wall temperatures and inclined plates with uniform heat flux, respectively. However, three-dimensional behavior and performance evaluation of mixed convection in an inclined channel have not been examined well.

In this study, authors analyzed numerically the heat transfer and three-dimensional flow behavior of mixed convection in a square channel with uniform wall temperatures, and evaluated thermal performance using Nusselt number ratio and pressure loss ratio with and without buoyancy induced flow.

2. Description of the problem

Mixed convection dominates the flow in a duct with heat removal from an electric device, in a solar collector tube or in a chan-

* Corresponding author.
E-mail address: ichimiya@yamanashi.ac.jp (K. Ichimiya).

0017-9310/$ - see front matter © 2008 Elsevier Ltd. All rights reserved.
doi:10.1016/j.ijheatmasstransfer.2008.10.016

Nomenclature

a	thermal diffusivity of fluid, m^2/s	T	temperature, °C, K
D	width of square channel, mm, m	T_b	mixed mean temperature of fluid, °C, K
g	acceleration of gravity, m/s^2	T_f	local fluid temperature, °C, K
Gr	Grashof number = $g\beta D^3(T_w - T_o)/\nu^2$	T_o	fluid temperature at the entrance, °C, K
h	heat transfer coefficient, $W/(m^2\,K)$	T_w	wall temperature, °C, K
Nu	Nusselt number = hD/λ	u,v,w	velocity along x, y, z, m/s
$\overline{Nu}$	average Nusselt number on each wall across the section	u_o	average fluid velocity at the entrance, m/s
$\overline{Num}$	mean Nusselt number along whole lengh	x,y,z	coordinate system
P	pressure, Pa	β	volume expansion coefficient, 1/K
ΔP	pressure difference between entrance and exit, Pa	λ	thermal conductivity of fluid, W/(mK)
Pr	Prandtl number, ν/a	ν	kinematic viscosity of fluid, m^2/s
Ri	Richardson number = Gr/Re^2	ρ	density of fluid, kg/m^3
t	time, s	θ	inclination angle

nel with chemical vapor deposition. The attitude of heat transfer section is one of the important factors, and we have to evaluate what attitude is effective for heat removal. Therefore, heat transfer and flow in a square channel with uniform temperature walls were analyzed numerically and basically for various inclination angles, and thermal performance including heat transfer and flow resistance was also evaluated.

Fig. 1 shows the coordinate system. Size of a square channel is a side $D = 20$ mm, length $l = 360$ mm including adiabatic entrance section 20 mm and θ inclination angle. The dimensionless entrance region le/D is usually estimated in laminar flow by 0.05 Re. In $Re = 100$, le/D is 5. In the present length of the channel is $l/D = 18$. Therefore, the channel length is assumed to be sufficient. Fluid temperature at the entrance is $T_0 = 10$ °C and wall temperature at heat transfer section is $T_w = 30$ °C. Gravity works downwards. Inclination angle, θ, is zero at horizontal plane, and $\theta > 0$ means rising flow of forced convection and on the other hand $\theta < 0$ means falling flow. Flow is fully developed at the entrance. Working fluid is incompressible viscous fluid (air). Physical properties of fluid are constant except for density. Buoyancy force is expressed by Boussinesq approximation and thermal radiation is neglected.

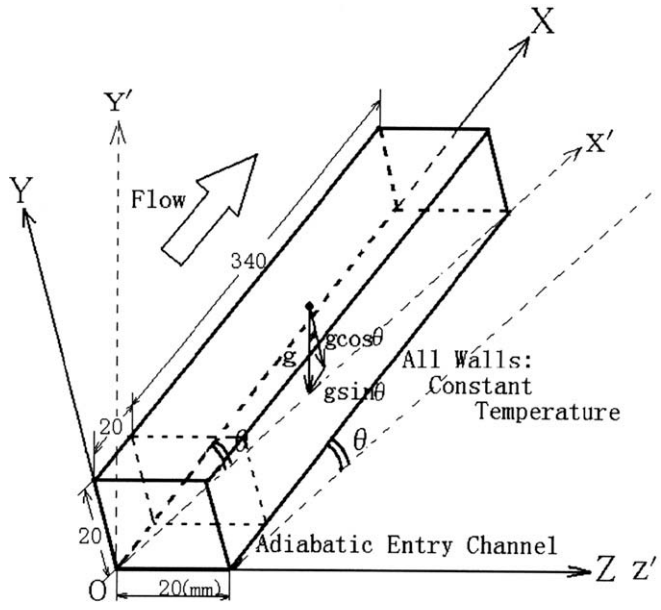

Fig. 1. Coordinate system.

3. Numerical analysis

Governing equations, conservation of mass, momentum and energy, are expressed as follows;

$$\frac{\partial u}{\partial x}+\frac{\partial v}{\partial y}+\frac{\partial w}{\partial z}=0 \tag{1}$$

$$\frac{\partial u}{\partial t}+u\frac{\partial u}{\partial x}+v\frac{\partial u}{\partial y}+w\frac{\partial u}{\partial z}=-\frac{1}{\rho}\frac{\partial p}{\partial x}+\nu\left(\frac{\partial^2 u}{\partial x^2}+\frac{\partial^2 u}{\partial y^2}+\frac{\partial^2 u}{\partial z^2}\right)-\beta(T-T_0)g\sin\theta \tag{2}$$

$$\frac{\partial v}{\partial t}+u\frac{\partial v}{\partial x}+v\frac{\partial v}{\partial y}+w\frac{\partial v}{\partial z}=-\frac{1}{\rho}\frac{\partial p}{\partial y}+\nu\left(\frac{\partial^2 v}{\partial x^2}+\frac{\partial^2 v}{\partial y^2}+\frac{\partial^2 v}{\partial z^2}\right)-\beta(T-T_0)g\cos\theta \tag{3}$$

$$\frac{\partial w}{\partial t}+u\frac{\partial w}{\partial x}+v\frac{\partial w}{\partial y}+w\frac{\partial w}{\partial z}=-\frac{1}{\rho}\frac{\partial p}{\partial z}+\nu\left(\frac{\partial^2 w}{\partial x^2}+\frac{\partial^2 w}{\partial y^2}+\frac{\partial^2 w}{\partial z^2}\right) \tag{4}$$

$$\frac{\partial T}{\partial t}+u\frac{\partial T}{\partial x}+v\frac{\partial T}{\partial y}+w\frac{\partial T}{\partial z}=a\left(\frac{\partial^2 T}{\partial x^2}+\frac{\partial^2 T}{\partial y^2}+\frac{\partial^2 T}{\partial z^2}\right) \tag{5}$$

Boundary conditions are established as follows;

(1) At the entrance, flow has fully developed laminar flow velocity distribution and fluid temperature is $T_0 = 10$ °C.
(2) Walls are uniformly heated at $T_w = 30$ °C after 20 mm adiabatic section.
(3) At the exit, the velocity gradient along x is zero, $\partial u/\partial x = 0$, $\partial v/\partial x = 0$, $\partial w/\partial x = 0$, and heat flux gradient is zero, $\partial^2 T/\partial x^2 = 0$.
(4) Initial conditions are that flow velocity distribution is fully developed at whole area and fluid temperature is $T_0 = 10$ °C.

Unsteady three-dimensional governing equations were reduced to systems of simultaneous algebraic equations by a control volume based on finite difference method. The velocity and pressure were obtained by SIMPLE algorithm [19], and the QUICK scheme [20] with the third order upwind method, was implemented to calculate the convection flux through the cell face of a control volume. The first operation involved solving the momentum equation using the upstream pressure gradient to correct the pressure and velocity profile. The velocity field was modified by a pressure correction technique to bring it in compliance with the conservation of mass. The cross sectional pressure distribution was evaluated by solving a Poisson equation for pressure. Code validation was accomplished through known results for forced convection [21] and numerical and experimental results for mixed convection in a horizontal duct

[22]. Grid independence test was performed by achieving sufficient agreement between results obtained for $20 \times 20 \times 360$, $30 \times 30 \times 360$ and $20 \times 20 \times 720$ [23]. As the result, the number of uniform staggered grids were $360(x) \times 20(y) \times 20(z) = 144{,}000$. The time step Δt was 0.005 s for numerical stability, and the state approached to steady condition at 7 s. Discussion was performed on numerical results at steady state. Calculation was performed at Prandtl number, $Pr = 0.72$, Reynolds number, $Re = 100$ and Richardson number, $Ri = 2.2$ and inclination angle, $\theta = -90°$ to 90°. Flow and heat transfer were evaluated by stream line, velocity vector, local and average Nusselt numbers.

The local Nusselt number is defined by

$$Nu = D(T_w - T_f)/\delta(T_w - T_b) \tag{6}$$

where δ is half distance of a grid size from the wall and T_f the fluid temperature at δ.

The local Nusselt number was averaged over one wall at arbitrary x and was determined by

$$\overline{Nu} = \sum_{k=1}^{n}[D(T_w - T_{fk})/\delta(T_w - T_b)]/n \tag{7}$$

where T_{fk} is the fluid temperature at k-th position of δ along the width and n the grid number on one wall. T_b is the mixed mean temperature of fluid and was determined by

$$T_b = \int_0^S T \cdot uds/u_m S \tag{8}$$

where u_m is average velocity across the section and S *cross-sectional area* ($= D^2$).In addition, $\overline{Nu}$ was averaged over the entire wall of the channel and was defined by

$$\overline{Num} = \sum_{k=1}^{4m}\overline{Nu_k}/4m \tag{9}$$

where m is the grid number along x-direction on one wall. Thermal performance was decided by average or local maximum Nusselt number ratio with and without buoyancy force for pressure difference between entrance and exit, $\overline{Num}/(\overline{Nu})_{g=0}$ or $Nu_{peak}/(Nu_f)_{g=0}$ against $\Delta P/(\Delta P)_{g=0}$, where $g = 0$ means forced convection.

4. Results and discussions

4.1. Flow characteristics

In order to examine the three-dimensional behavior, flow streak lines from $x = 0$, $z = 5$ mm and $y = 4$, 8, 12, 16 mm are shown for various inclination angles in Fig. 2. In $\theta = 0°$, fluid rises up near the bottom wall due to wall heating, and on the other hand it falls

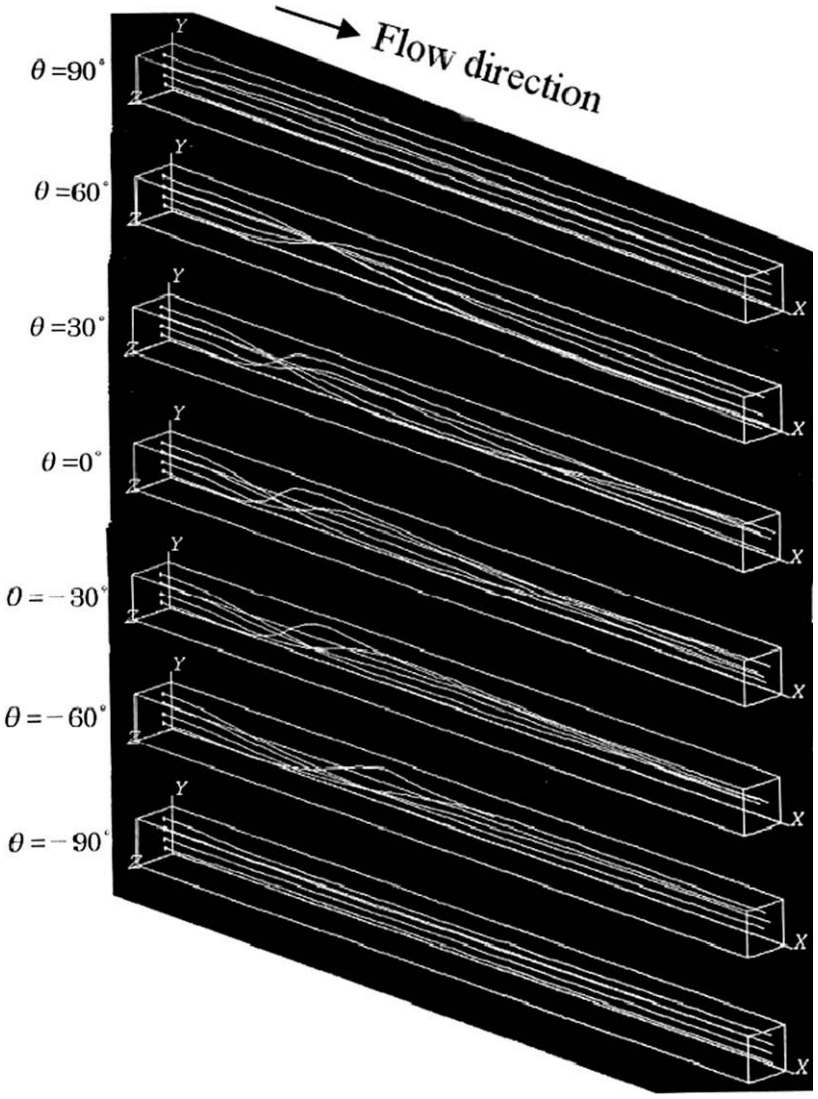

Fig. 2. Streak lines.

down near the upper wall. Therefore, it flows downstream with twisting [23]. The gradient of streak lines along the flowing direction becomes mild with increase of inclination angle. In $\theta = 90°$, the direction of the buoyancy flow agrees with that of forced convection and the flow is accelerated near the wall. In negative inclination angle, the flow is decelerated near the wall because the direction of the buoyancy flow is opposite to that of forced convection (refer to Fig. 5).

Fig. 3 shows the velocity vector across the section at $x = 80$mm. Flow is divided into two recirculating flows, namely, rising flow

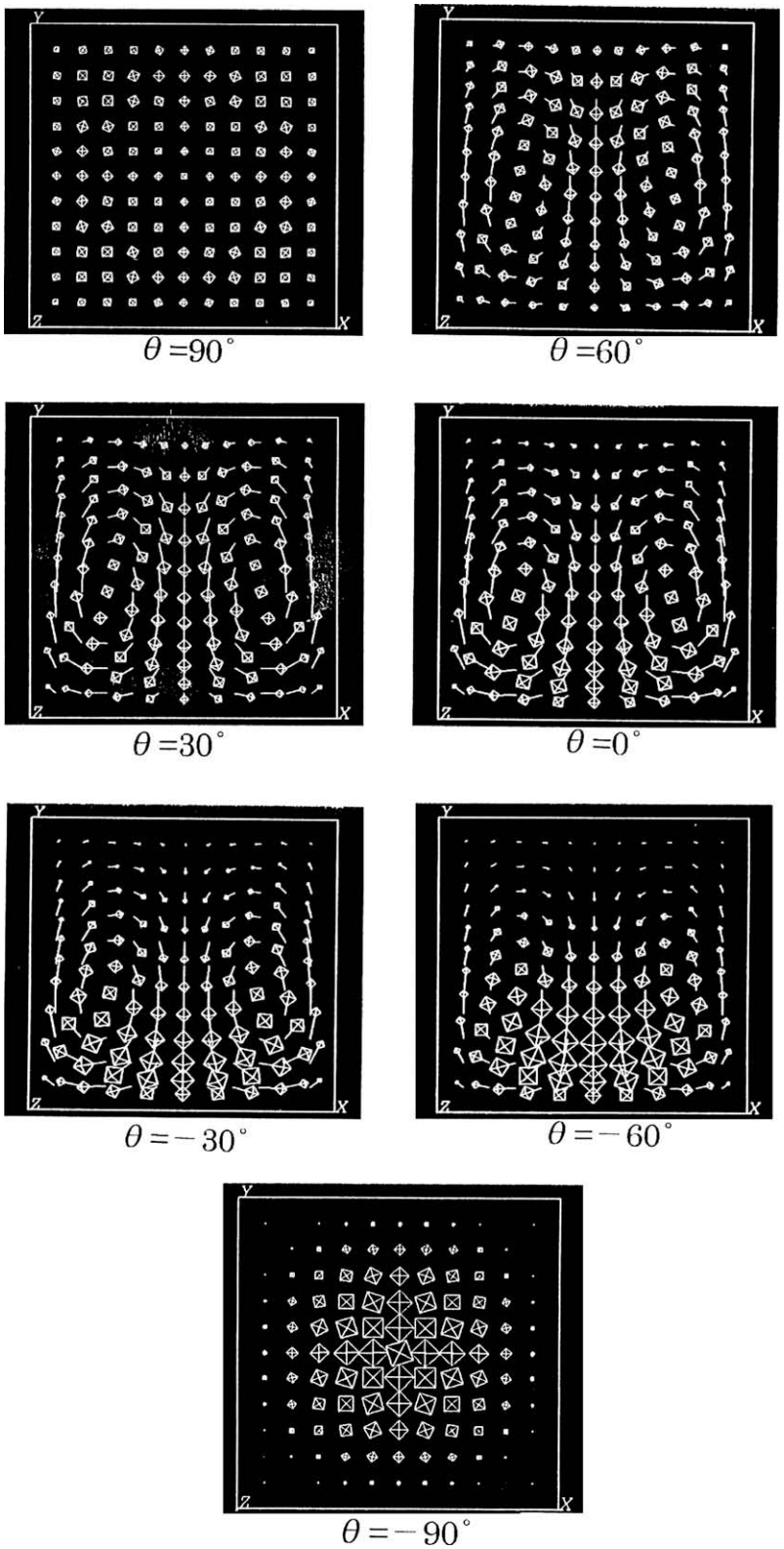

Fig. 3. Velocity vectors at $x = 80$ mm.

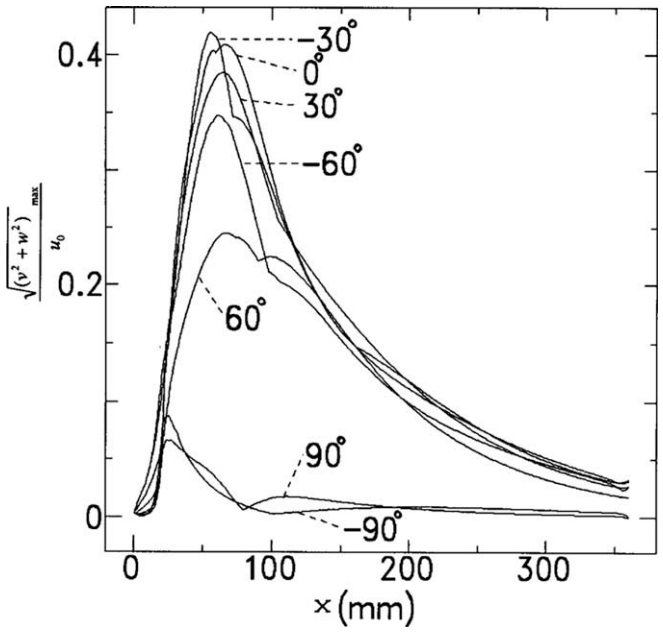

Fig. 4. Intensity of maximum secondary flow.

along side wall and falling flow near the center of the flow passage. The center of the recirculating flow moves to upper wall and the flow is accelerated near the wall with increase of inclination angle. In $\theta = 90°$, velocity distribution becomes more uniform or is relatively decelerated at the center of flow passage and becomes concave. In negative inclination angle, the center of recirculating flow moves toward bottom wall and velocity is accelerated near the bottom wall. In the inclination angle close to $\theta = -90°$, main flow and inverse buoyancy flow becomes strong and flow is decelerated near the wall. Therefore, velocity distribution becomes convex due to the acceleration near the center of the flow passage (refer to Fig. 5).

Fig. 4 presents the intensity of the maximum secondary flow across the section defined by $(\sqrt{(v^2+w^2)_{max}}/u_o)$ along the flow direction for various inclination angles. The intensity increases generally from the starting point of heat transfer, takes a peak corresponding to the rise or fall of streak lines shown in Fig. 2, and after that it decreases along the flow direction. Between $\theta = -30°$ and $\theta = 30°$, the intensity behaves in the same way along the flow direction. In $\theta = 90°$ and $\theta = -90°$, it becomes low due to the positive or negative buoyancy induced flow corresponding to main flow. After the first peak of the intensity, there exists the region where the second peak can be found or the gradient along the flow direction changes. This behavior corresponds to the cross portion

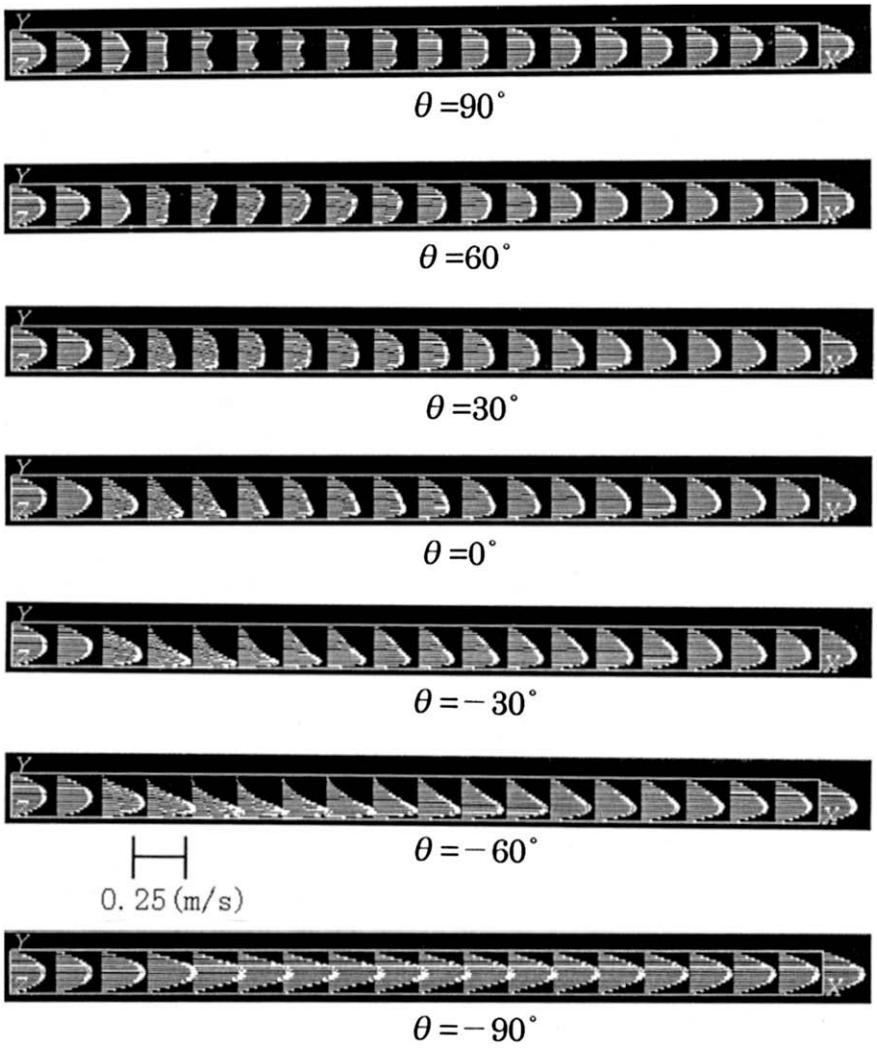

Fig. 5. Velocity distribution along x–y cross section at $z = 10$ mm.

of rising and falling streak lines in Fig. 2. In $\theta = 90°$, these streak lines do not cross. However, the area is where the flow near the wall is accelerated due to buoyancy flow and is decelerated near the center of the flow passage, and the velocity distribution becomes concave as shown in Fig. 5.

4.2. Heat transfer characteristics

Temperature distributions across (y–z) section at $x = 80$ mm are shown for $\theta = 60°$ and $\theta = -60°$ in Fig. 6. High temperature region near the wall exists, and low temperature region exists at lower section for $\theta = -60°$ comparing with that for $\theta = 60°$ and high temperature region becomes wide at upper section. Temperature gradient near the lower wall becomes high corresponding to the flow acceleration near the lower wall and flow deceleration at upper section for $\theta = -60°$. The present tendency near the lower wall becomes remarkable at close to $\theta = 0°$.

Fig. 7 shows the local Nusselt numbers on the lower wall for $\theta = 30°$ and $\theta = -60°$. In lower absolute value of inclination angle, local Nusselt number becomes high (Fig. 10) because low tem-

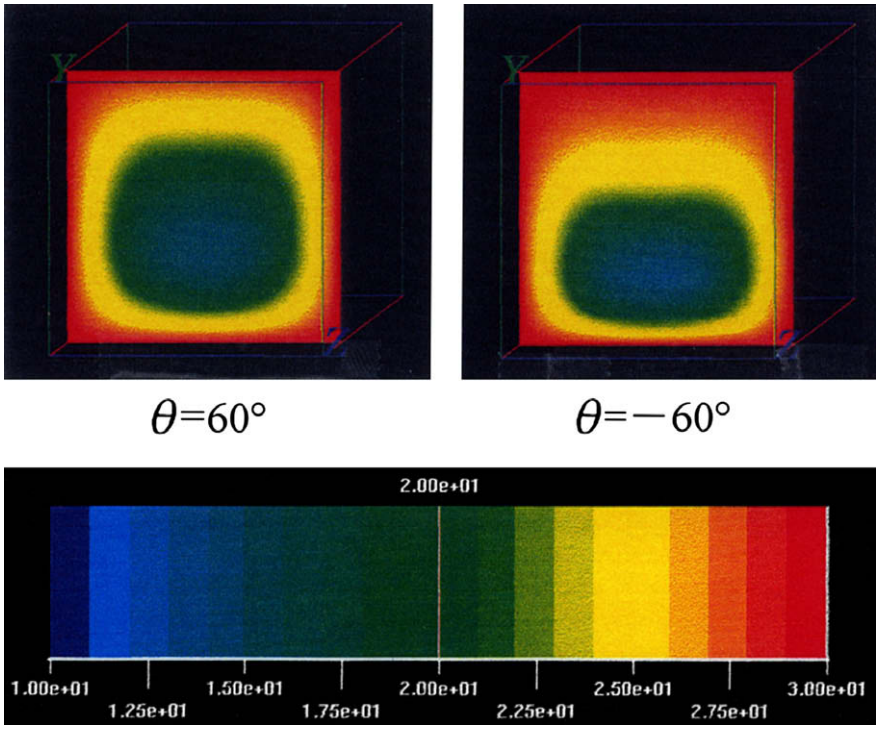

Fig. 6. Fluid temperature across (y–z) ($x = 80$ mm).

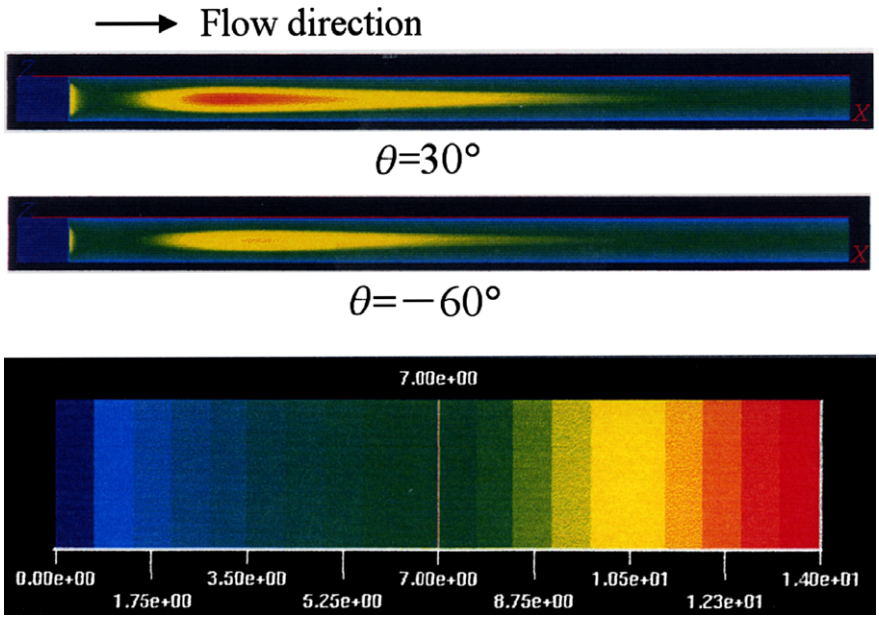

Fig. 7. Local Nusselt number on the bottom wall.

perature fluid near the upper wall falls down and impinges the lower wall. That is why local heat flux increases, and this state expands downstream. The average Nusselt number on each wall across the section is presented along flow direction in Figs. 8–10. The average Nusselt number on the upper wall shown in Fig. 8 takes the minimum in a certain position at wide high temperature region as shown in Fig. 6 and after that it increases downstream. The value is the lowest at $\theta = -60°$ and the highest for $\theta = 90°$ due to flow acceleration. In $\theta = -90°$ and $\theta = 90°$, the flow is symmetrical and the average Nusselt numbers have same distributions at upper wall, side wall and lower wall, respectively. Fig. 9 shows the average Nusselt number on side wall. Flow along the side wall generally rises up to upper wall and average Nusselt number takes maximum at $x = 90$ mm for $\theta = 30°$. The position moves downwards with inclination angle and the behavior becomes mild. The flow becomes mild with larger inclination angle than $\theta = 30°$ and the peak does not exist. Fig. 10 shows average Nusselt number on lower wall. It takes sharp peak at $x = 85$ mm for $\theta = 0°$. This tendency is same as at the region $\theta = -30°$ to 30°. In $\theta = -60°$, the temperature gradient on the lower wall is higher than that in $\theta = 60°$ and average Nusselt number is higher. Generally, it is high at negative inclination angle. However, in $\theta = -90°$, flow is decelerated near the wall due to buoyancy force, and heat transfer is depressed for low temperature gradient comparing with that at $\theta = 90°$.

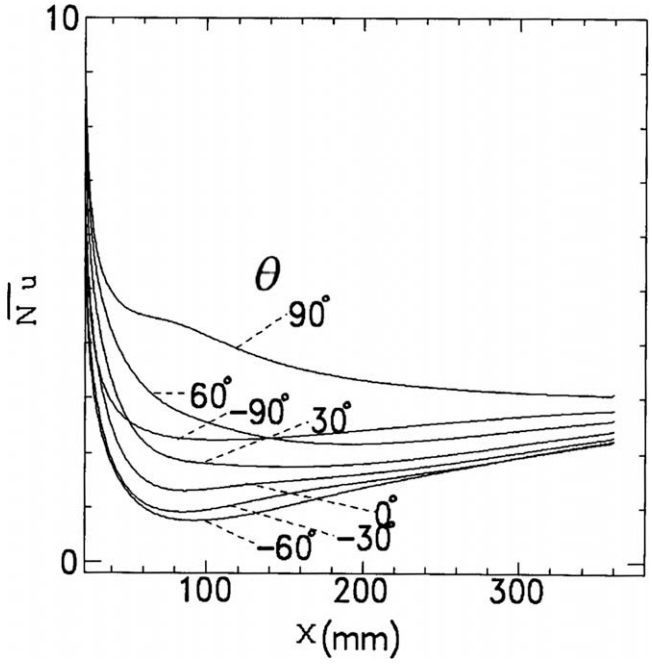

Fig. 8. Average Nusselt number on the upper wall along flow direction.

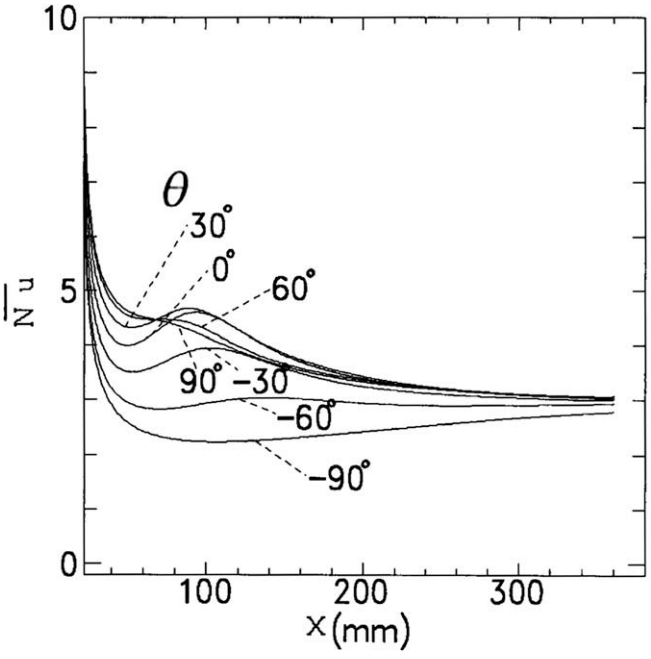

Fig. 9. Average Nusselt number on the side wall along flow direction.

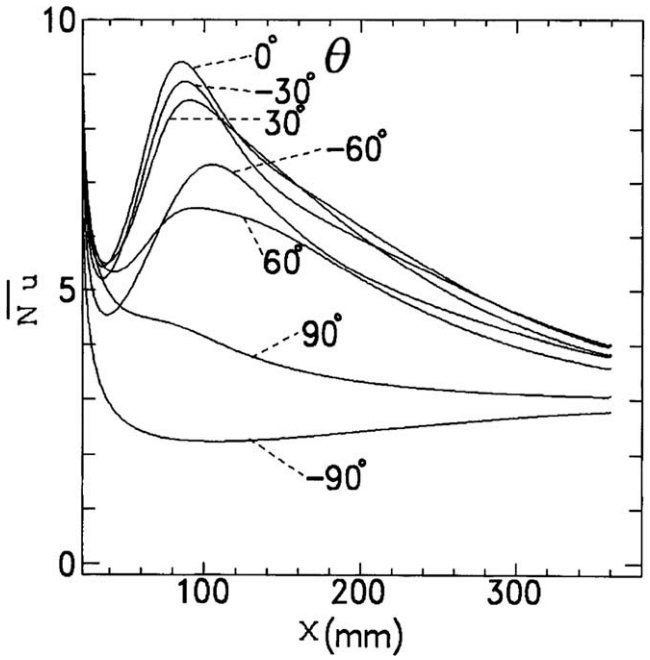

Fig. 10. Average Nusselt number on the bottom wall along flow direction.

4.3. Thermal performance

Two kinds of thermal performance were determined by the mean Nusselt number ratio along whole length and the local maximum Nusselt number ratio against pressure difference ratio between entrance and exit with and without buoyancy force. These were indicated in Figs. 11 and 12. The 45° dotted line means that Nusselt number ratio is same as pressure difference ratio. In Fig. 11, mean Nusselt number ratio $\overline{Num}/(\overline{Nu})_{g=0}$ is higher and pressure difference ratio $\Delta P/(\Delta P)_{g=0}$ is lower than 1.0 for $\theta = -15°$ to $-60°$. This means high heat transfer and low pressure loss area. The $\theta = -60°$ to $-90°$ region is low heat transfer and low pressure loss area because of both lower values than 1.0. The $\theta = -15°$ to 30° region is high heat transfer and high pressure loss area, and heat transfer dominates due to higher $\overline{Num}/(\overline{Nu})_{g=0}$ than dotted line. The $\theta = 30°$ to 90° region is high heat transfer and high pressure loss area, and pressure loss dominates the field because $\overline{Num}/(\overline{Nu})_{g=0}$ < dotted line. Consequently, thermal performance is divided into four regions. In Fig. 12, maximum Nusselt number ratio $Nu_{peak}/(Nu_f)_{g=0}$ is higher than dotted line except for $\theta = 90°$ and heat transfer dominates the field. In the $\theta = -15°$ to $-90°$ region, Nusselt number ratio is higher than 1.0 and pressure difference ratio is less than 1.0. Therefore, it is high heat transfer and low

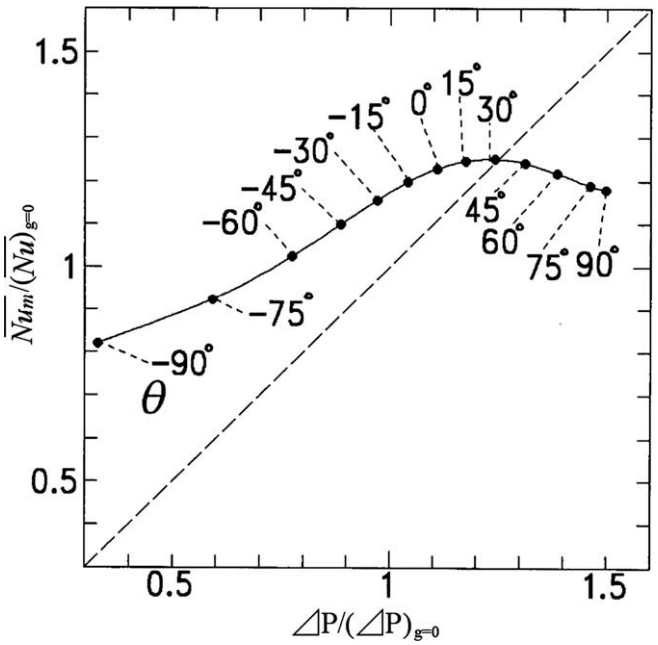

Fig. 11. Thermal performance by mean Nusselt number.

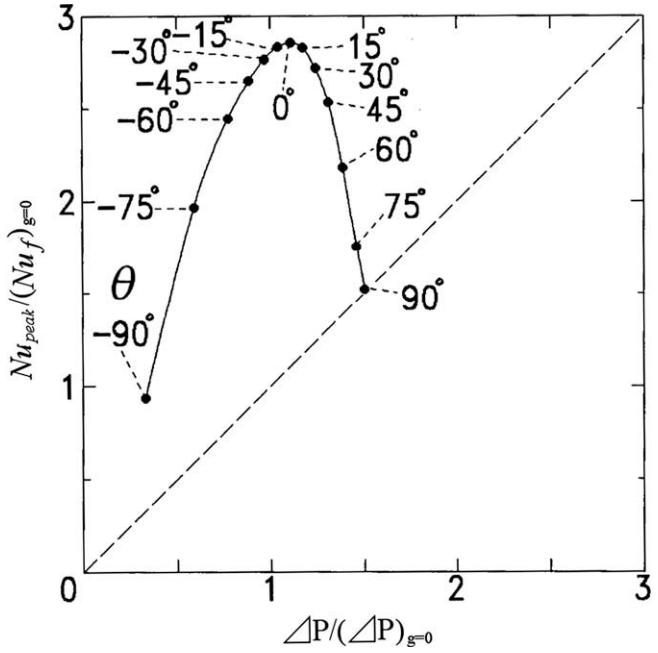

Fig. 12. Thermal performance by peak Nusselt number.

pressure loss region. On the other hand, the $\theta = -15°$ to 90° region is high heat transfer and high pressure loss area and heat transfer dominates because $Nu_{peak}/(Nu_f)_{g=0}$ is higher than dotted line. Consequently, thermal performance is divided into two-regions. These results show that the thermal performance depends on inclination angle. We should select the inclination angle in accordance with practical objectives.

5. Conclusion

Effect of attitude of flow passage on heat transfer and flow of mixed convection in a square channel with uniform temperatures walls was analyzed numerically for $-90 \leqslant \theta \leqslant 90°$ and thermal performance was evaluated. Following conclusions are obtained;

(1) Three-dimensional flow is basically composed of twisted flow by rising flow along side walls and falling flow along the center of the flow passage.
(2) The flow across the section generates two-big recirculating flows except for $\theta = 90°$ and –90° and the center of recirculating flow moves upward of flow passage for positive inclination angle and moves downwards for negative inclination angles.
(3) Thermal performance was evaluated by relationship between mean Nusselt number ratio and pressure difference ratio with and without buoyancy force. High heat transfer and low pressure loss area was obtained for $\theta = -15°$ to $-60°$, and other regions were divided into three.
(4) Other thermal performance was evaluated by the relationship between maximum Nusselt number ratio and pressure loss ratio with and without buoyancy force. High heat transfer and low pressure loss area was obtained for $\theta = -15°$ to $-90°$, and other region was divided into one.

References

[1] M. Iqbal, J.W. Stachiewicz, Influence of tube orientation on combined free and forced laminar convection heat transfer, Trans. ASME C 88 (1966) 109–116.
[2] J.R. Maughan, F.P. Incropera, Experiments on mixed convection heat transfer for airflow in a horizontal and inclined channel, Int. J. Heat Mass Transfer 30 (1987) 1307–1318.
[3] N. Ramachandran, B.F. Armaly, T.S. Chen, Measurement of laminar mixed convection flow adjacent to an inclined surface, Trans. ASME C 109 (1987) 146–150.
[4] E. Naito, Y. Nagano, Combined forced and free upward-flow convection in the entrance region between inclined parallel plates, Trans. ASME C 111 (1989) 146–150.
[5] G. Wikem, Mixed convection from an arbitrary inclined semi-infinite flat plate (part 1, the influence of inclination angle), Int. J. Heat Mass Transfer 34 (1991) 1935–1945.
[6] C.Y. Choi, A. Ortega, Mixed convection in an inclined channel with a discrete heat source, Int. J. Heat Mass Transfer 36 (1993) 3119–3134.
[7] X. Wang, L. Robillard, Mixed convection in an inclined channel with localized heat sources, Numer. Heat Transfer A 28 (1995) 355–373.
[8] W.M. Yan, Transport phenomena of developing laminar mixed convection heat and mass transfer in inclined rectangular ducts, Int. J. Heat Mass Transfer 38 (1995) 2905–2914.
[9] O.M. Galanis, Effects of wall and non-uniform thermal condition on developing flow with mixed convection in an inclined tube, Int. J. Them. Sci. 38 (1999) 622–633.
[10] H.I. Abu-Mulawech, B.F. Armaly, T.S. Chen, Instabilities of mixed convection flows adjacent to inclined plates, Trans. ASME C 109 (1987) 1031–1033.
[11] S.L. Lee, T.S. Chen, B.F. Armaly, Non-parallel wave instability of mixed convection flow on inclined flat plates, Int. J. Heat Mass Transfer 31 (1988) 1385–1398.
[12] A.S. Lavine, On the linear stability of mixed and free convection between inclined parallel plates with fixed heat flux boundary conditions, Int. J. Heat Mass Transfer 36 (1993) 1373–1387.
[13] O.J. Galanis, C.T. Nguyen, Bifurcation steady laminar mixed convection flow in uniformly heated tubes, Int. J. Numer. Methods Heat Fluid Flow 9 (1999) 543–567.
[14] A.S. Lavine, M.Y. Kim, C.N. Shores, Flow reversal in opposing mixed convection flow in inclined pipes, Trans. ASME C 111 (1989) 114–120.
[15] W.L. Lin, T.F. Lin, Observation and computation of vortex and/or reverse flow development in mixed convection of air in a slightly inclined rectangular duct, Trans. ASME C 119 (1997) 691–699.
[16] S.M. Morcos, M.M. Hilal, M.M. Kamel, M.S. Soliman, Experimental investigation of mixed laminar convection in the entrance region of inclined rectangular channels, Trans. ASME C 108 (1986) 574–579.
[17] T.S. Chen, B.F. Armaly, N. Ramachandran, Correlation for laminar mixed convection flows on vertical inclined and horizontal flat plates, Trans. ASME C 108 (1986) 835–840.
[18] B.F. Armaly, T.S. Chen, N. Ramachandran, Correlations for laminar mixed convection on vertical, inclined and horizontal flat plates with uniform surface heat flux, Int. J. Heat Mass Transfer 30 (1987) 405–408.
[19] S.V. Patankar, Numerical Heat Transfer and Fluid Flow, vol. 126, Hemisphere Publishing Corp., London, 1980.
[20] B.P. Leonard, Computer Methods in Fluids, vol. 159, Pentech Press, Plymouth, 1980.

[21] R.K. Shah, A.L. London, Laminar forced convection in ducts, in: T.F. Irvine, J.P. Hartnett (Eds.), Advanced in Heat Transfer, Academic Press, New York, 1978, pp. 196–222 (supplement 1).
[22] Y. Sakamoto, T. Kunugi, K. Ichimiya, Experimental and numerical flow visualization of mixed convection with flow reversal in a horizontal isothermal channel, in: Proceedings of Transport Phenomena in Thermal Science and Process Engineering, vol. 2, 1997, pp. 535–539.
[23] T. Kunugi, K. Ichimiya, Y. Sakamoto, Numerical analysis of mixed convective heat transfer in a square channel with uniform wall temperature, Trans. JSME B 60 (1994) 1393–1400.